Renal deposition and clearance of recombinant poly-IgA complexes in a model of IgA nephropathy

X Xie *et al. J Pathol* DOI: 10.1002/path.5658

Supplementary Figures S1–S16

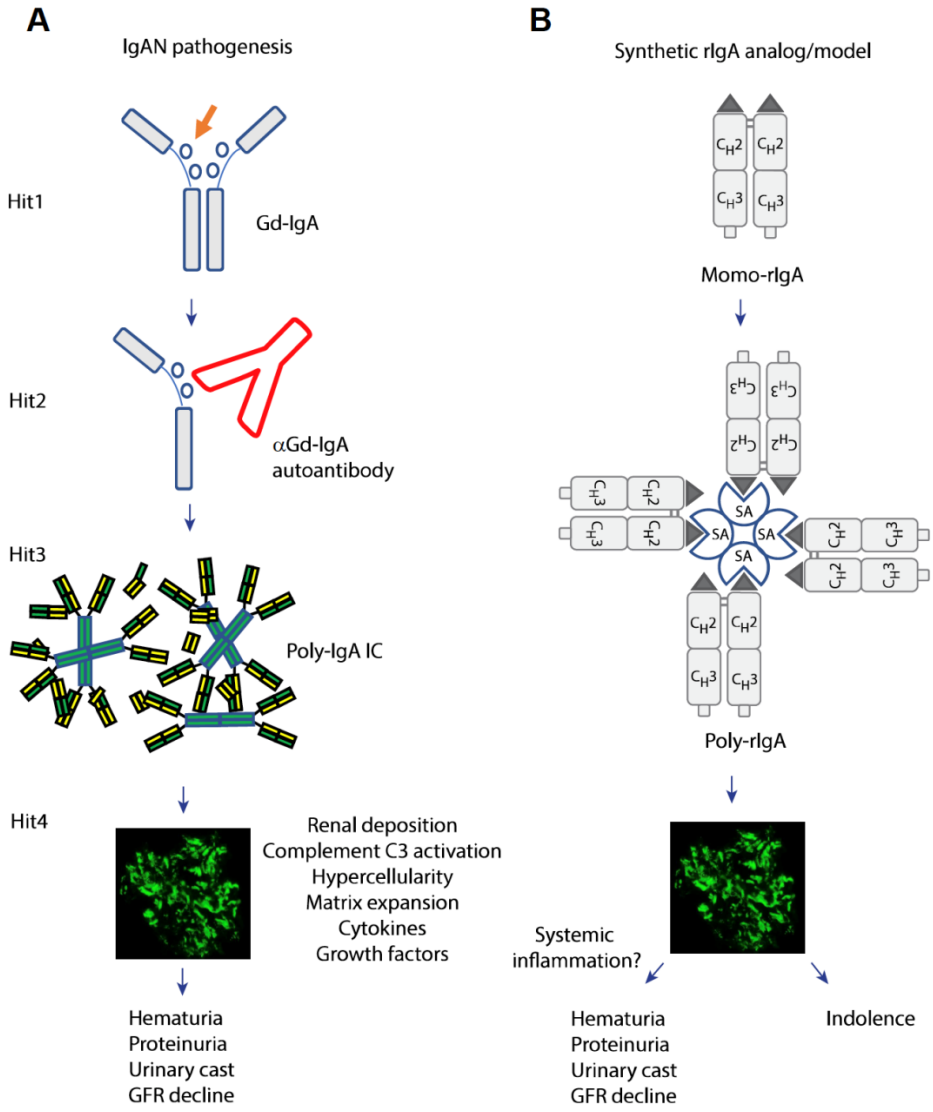

Figure S1. A schematic comparison of naturally formed poly-IgA1 in IgAN and synthetic poly-rIgA analog in this study.
(A) In the 4-hits hypothesis, aberrantly glycosylated Gd-IgA1 is the root cause of IgAN. It has an intrinsic tendency to form protein aggregates and may induce antiglycan IgG autoantibodies in forming IgA1–IgG complexes. These poly-IgA1 complexes ultimately deposit in the glomerulus, causing inflammation and renal damage. (B) In contrast, we constructed recombinant fusions between IgA Fc (CH2/CH3) and biotin. This rIgA analog can be induced to form high-order oligomers by adding streptavidin (SA). This poly-rIgA, not its uninduced mono-rIgA counterpart, formed glomerular deposits in the kidney that resembled many of the clinical manifestations of IgAN.

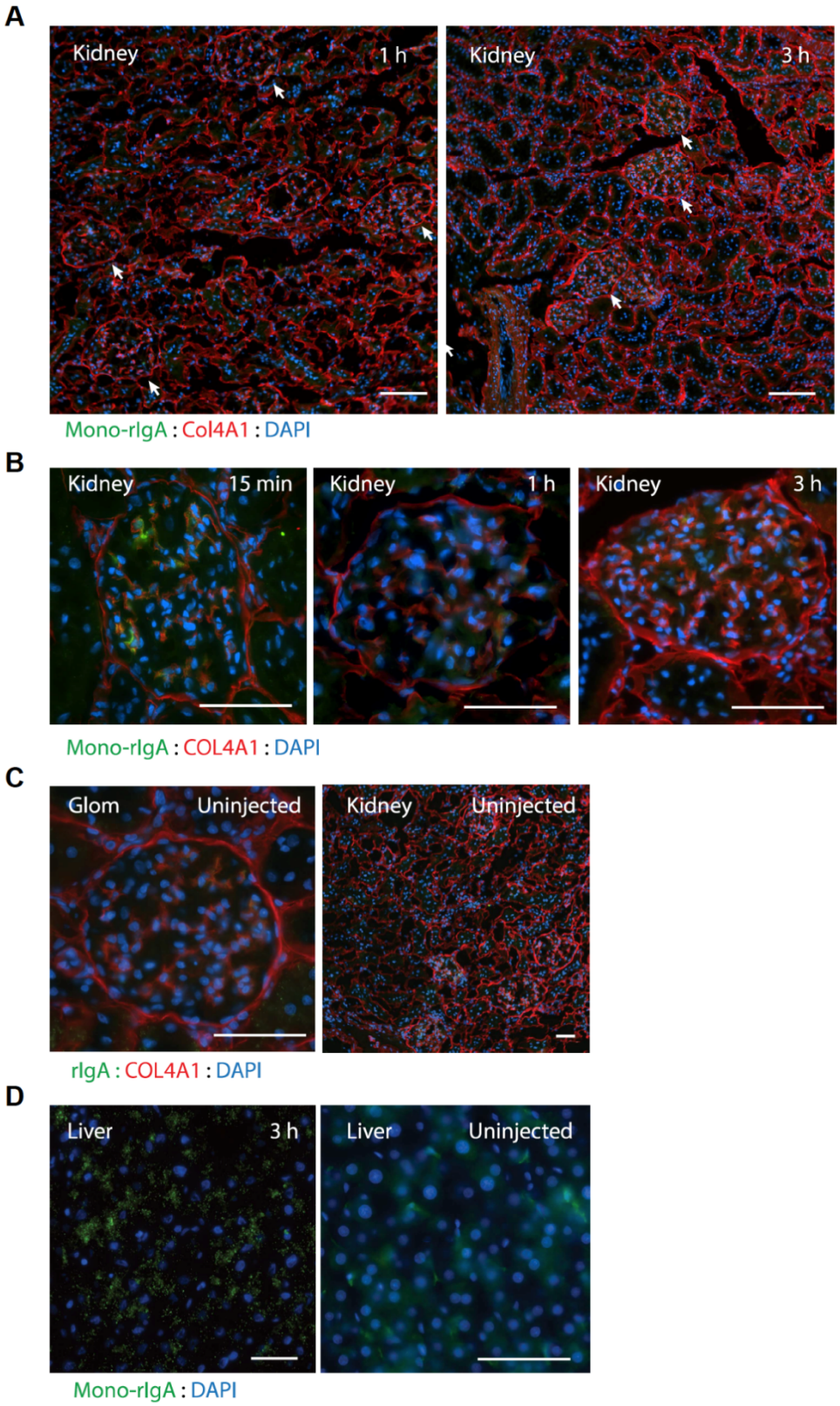

Figure S2. Injection of mono-rIgA in rats did not form renal deposits.
(A, B) As in Figure 2, 15 min, 1 h, and 3 h following the injections, kidneys were harvested for immunofluorescence detection of rIgA. Little to no mono-rIgA signal was present in the kidney. (C) Non-injected control. (D) Liver staining after bolus mono-rIgA injection and a non-injected control.

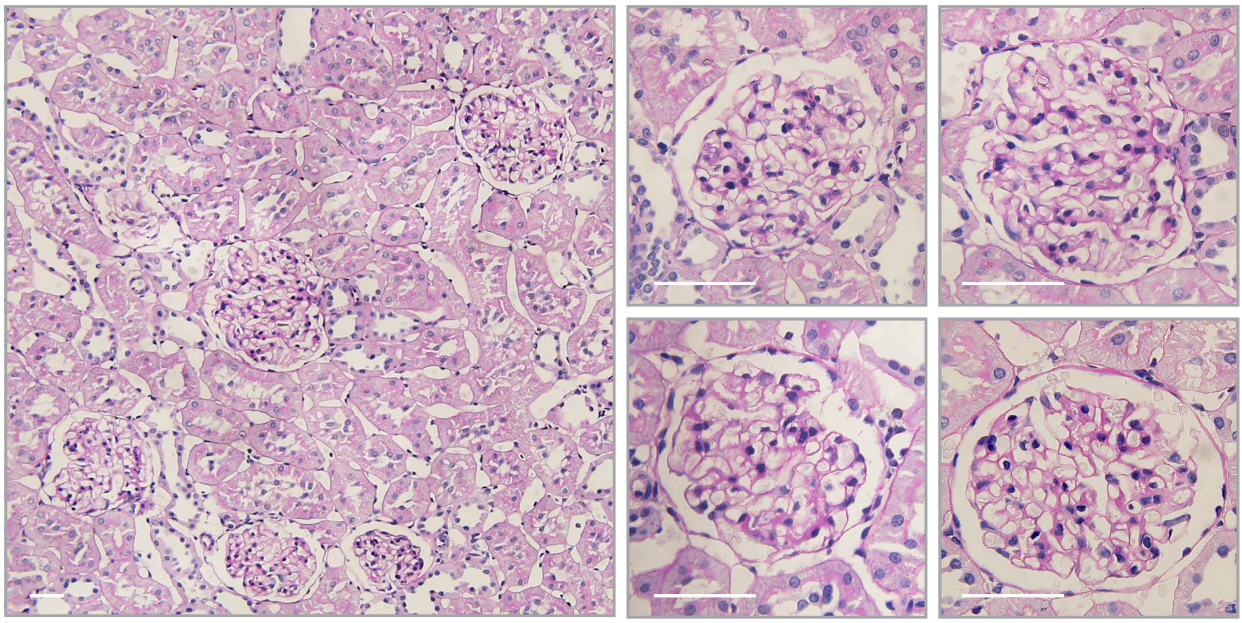

Figure S3. Normal renal histology following a single dose of injected poly-rIgA.
Normal glomeruli and tubular interstitium were found in rats after one dose of injected Poly-rIgA. Scale bar: 50 μm.

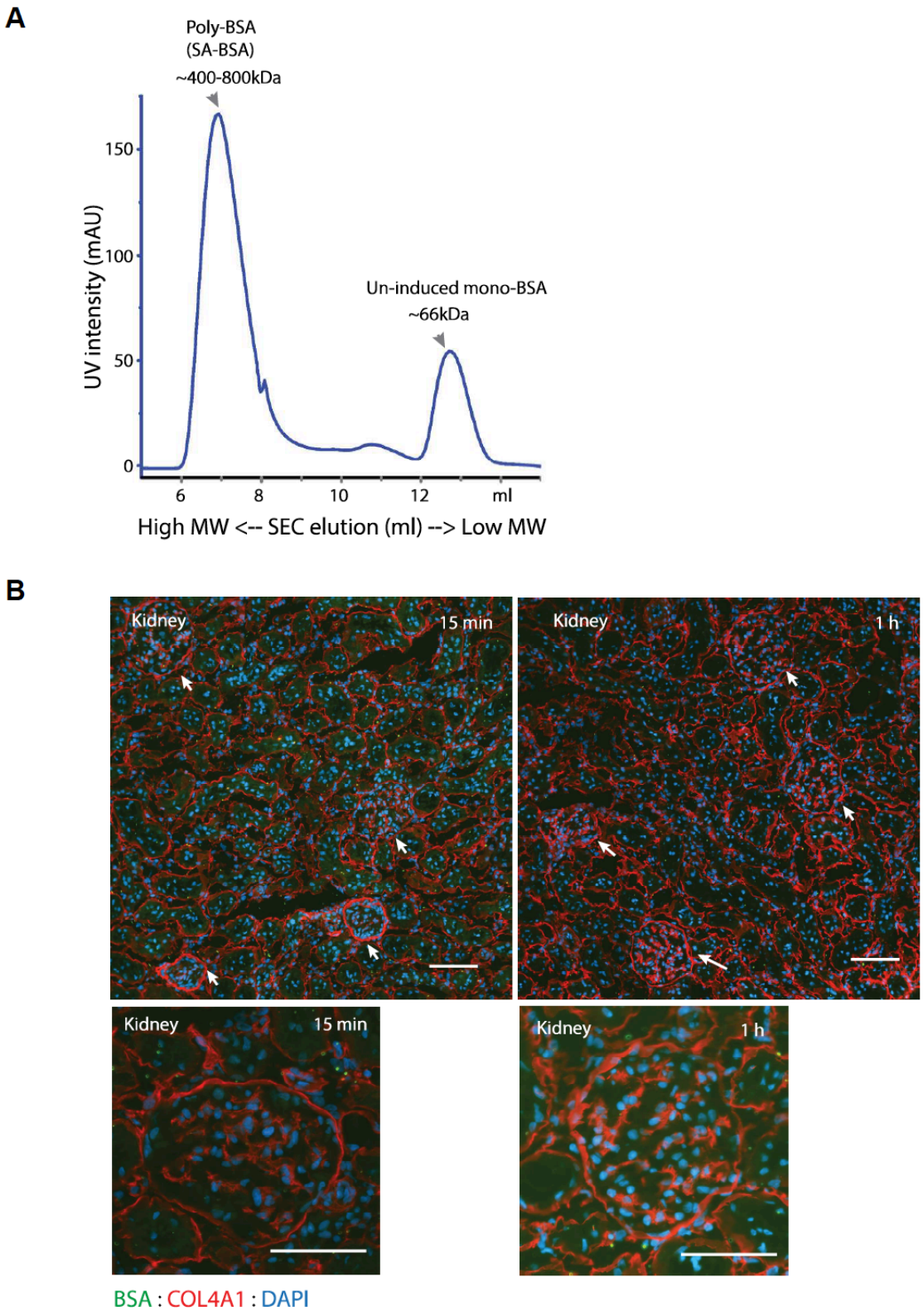

Figure S4. Streptavidin (SA) induction of poly-BSA (SA-BSA) did not form renal deposits.
(A) Biotinylated BSA protein with the presence or absence of streptavidin was analyzed by size exclusion chromatography. An apparent upshifting of the overall molecular weight was seen for the streptavidin-induced sample. (B) Rats were injected with 2 mg/kg SA-BSA complexes. Kidneys were collected after 15 min and 1 h. The sections were stained with an anti-BSA antibody and no BSA deposits were observed. Scale bar: 50 μm.

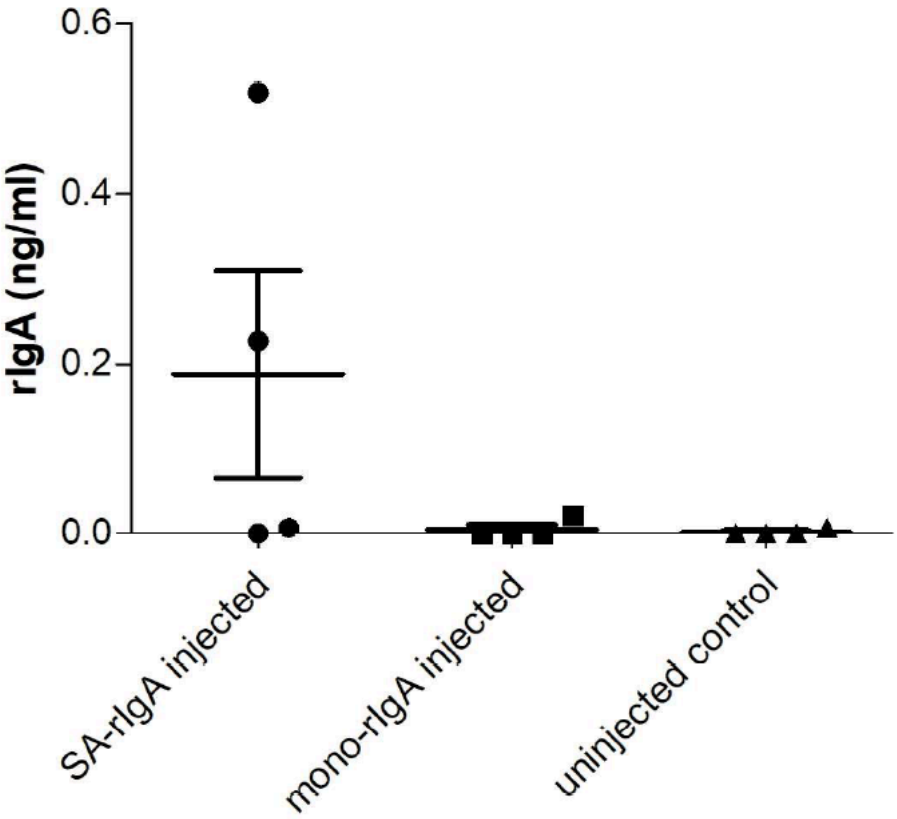

Figure S5. Urinary rIgA levels following poly-rIgA (SA-rIgA) or mono-rIgA injection in rats.
Urine samples were collected between 4 and 24 h after SA-rIgA or mono-rIgA injection. rIgA levels in most samples were undetectable. The highest rIgA concentration in urine was only 0.5 ng/ml and in one rat that received SA-rIgA.

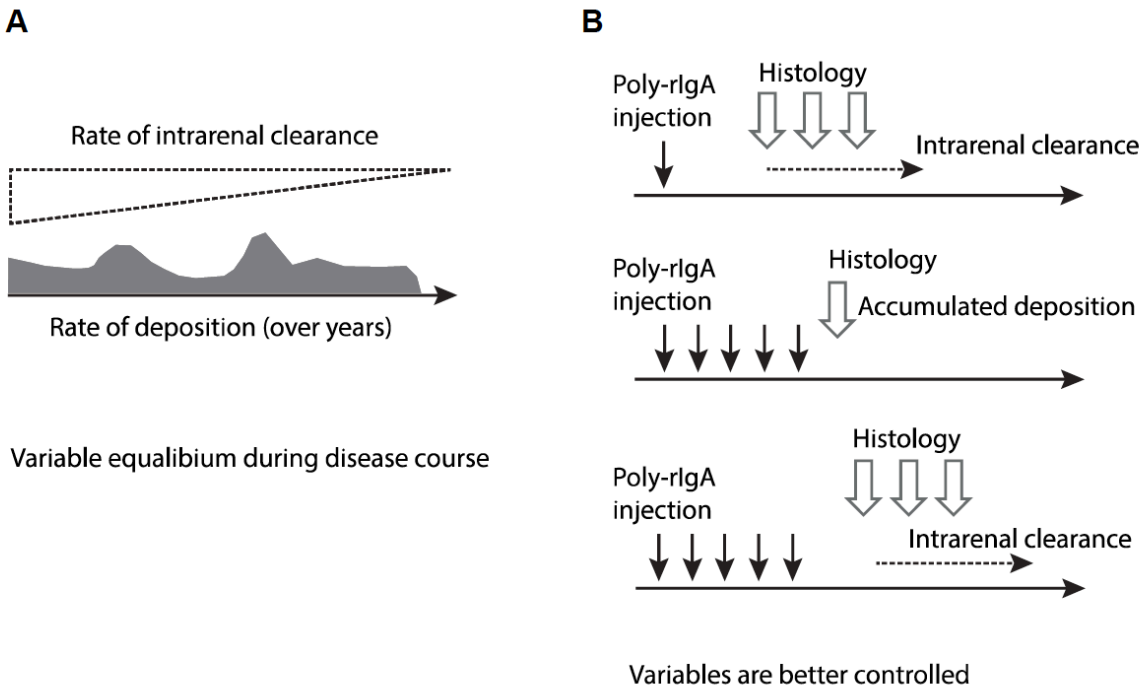

Figure S6. Schematics of mesangial IgA deposits during the years-long disease course of IgAN versus a short period of poly-rIgA injection model in the current study.
(A) The clinical course of IgAN follows chronic progression with flare-up episodes after infections. The dynamics of intrarenal clearance of deposits are unknown (broken triangle). (B) The synthetic model allows study of these dynamics with regard to the rate of deposition and clearance in a controlled manner.

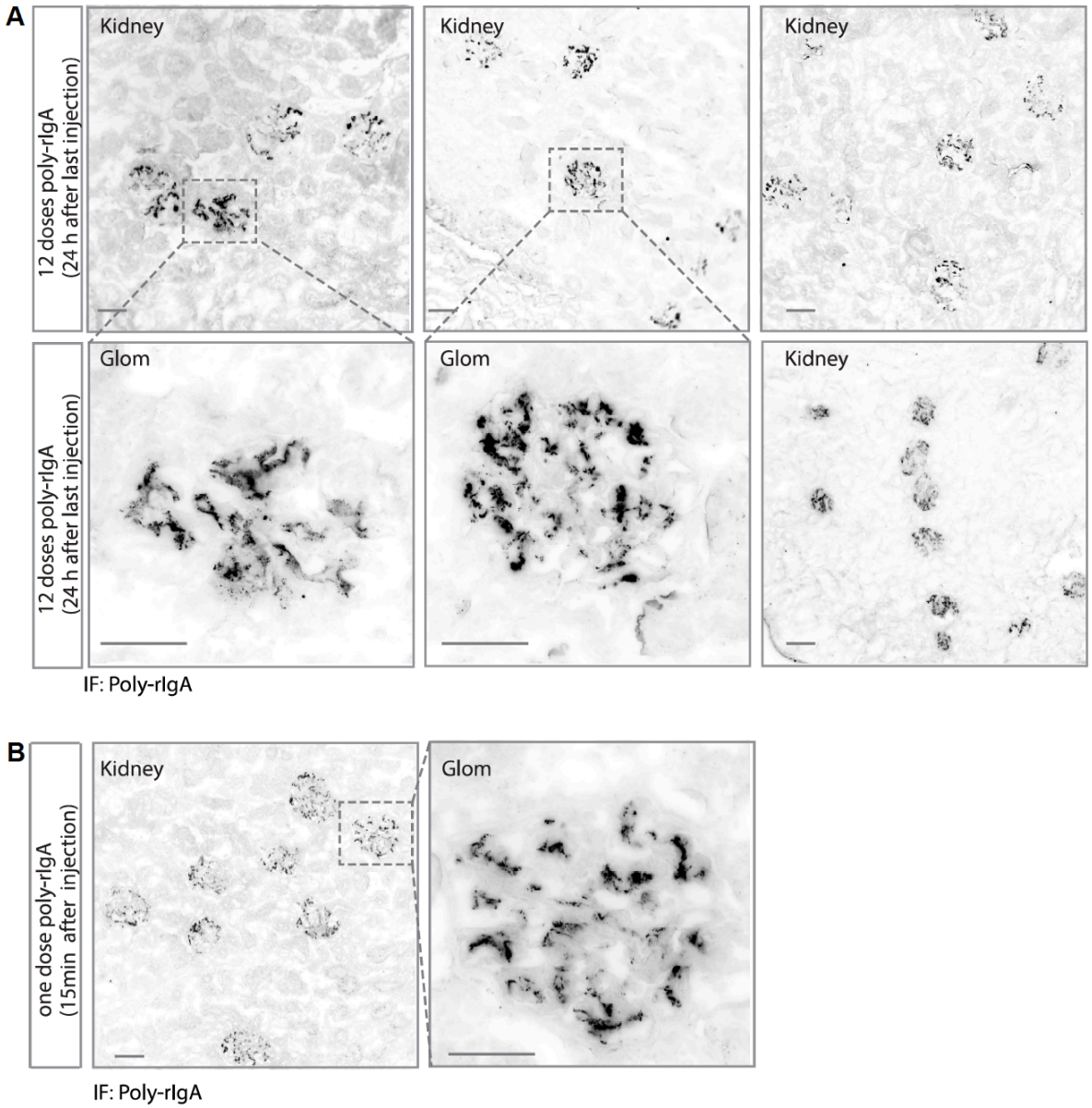

Figure S7. Immunofluorescence staining of poly-rIgA deposits in the kidney.
(A) After 12 consecutive doses of injected poly-rIgA. Insets show mesangial and capillary wall deposits. (B) Renal poly-rIgA deposits following single bolus injections. One of the glomeruli seen here at low magnification is shown at higher magnification in Figure 2G as another example.

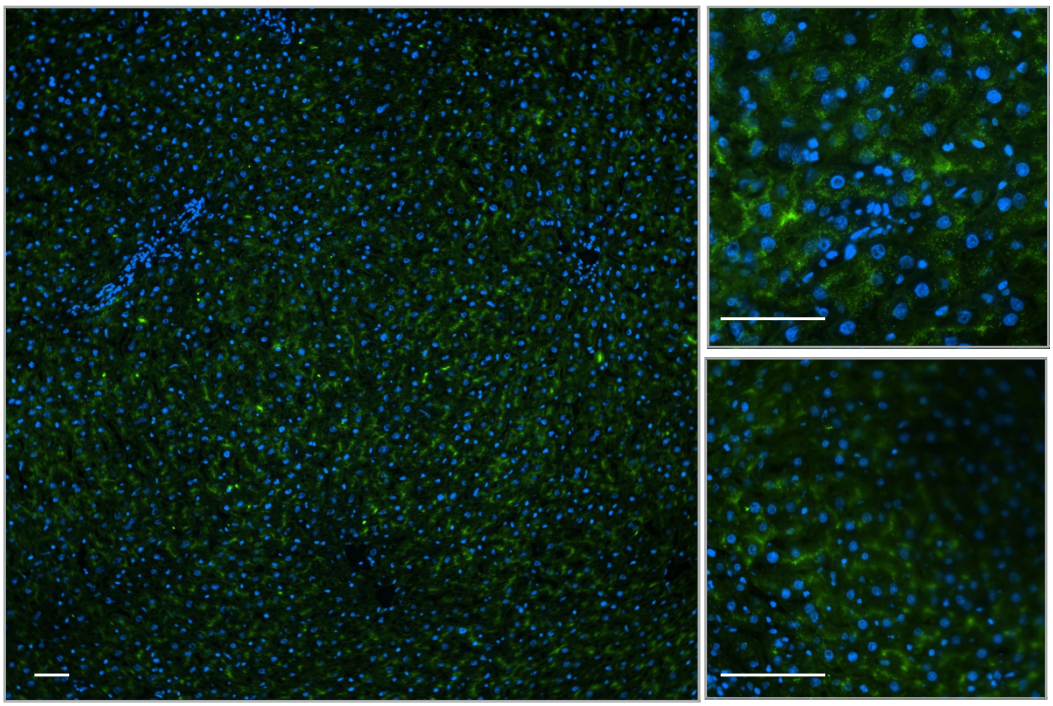

Figure S8. Trace IgA deposits in the liver 24 h following 12 consecutive doses of injected poly-rIgA. Scale bar: 50 μm.

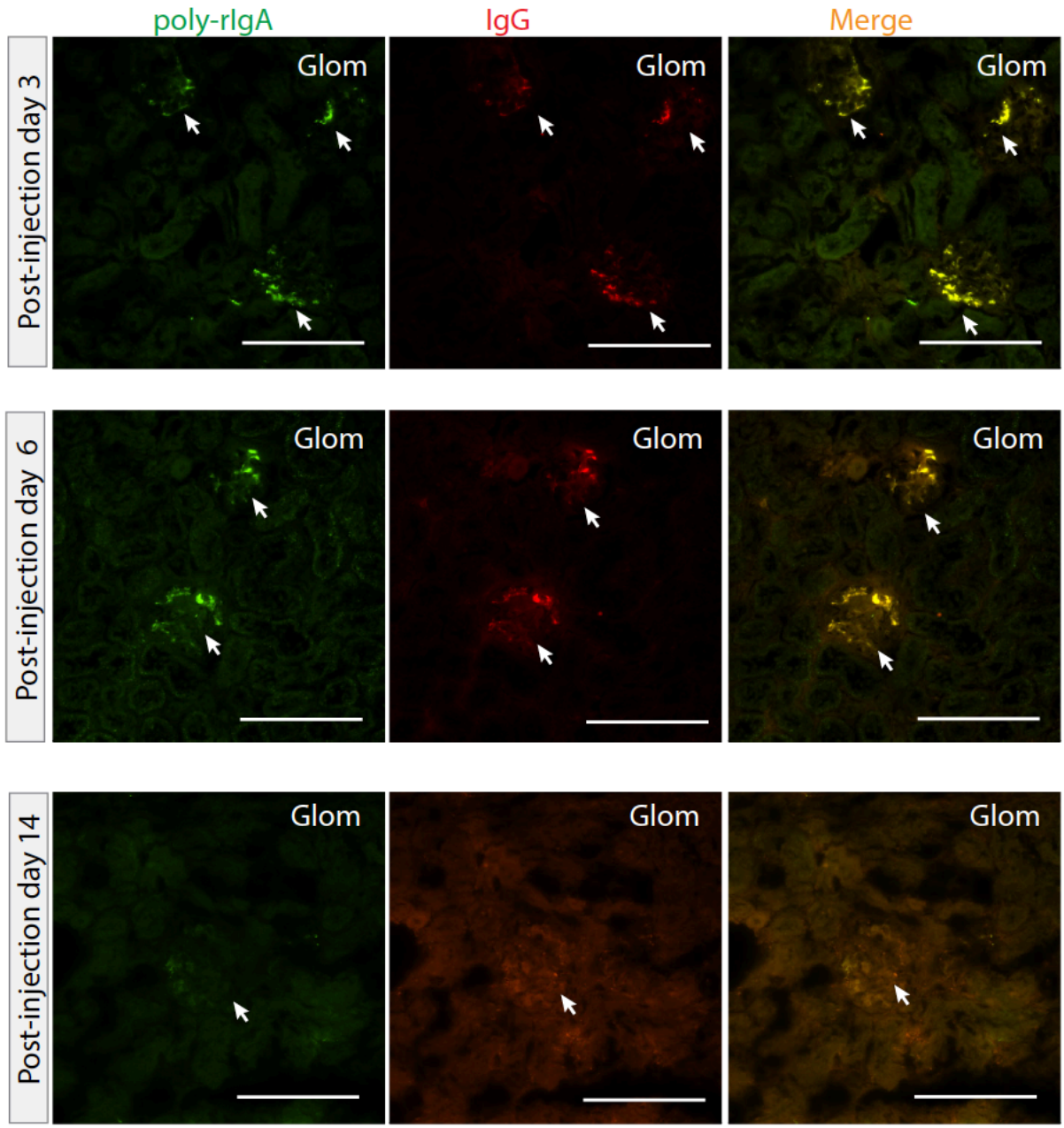

Figure S9. Time-dependent clearance of IgG co-deposition in rat kidney.
Following 12 consecutive daily doses of poly-rIgA, rats were allowed to recover for 3, 6 or 14 days. On days 3 and 6, poly-rIgA and IgG co-deposits were visible in the glomeruli (arrows). By day 14, both poly-rIgA and IgG staining had disappeared. Scale bar: 5 µm.

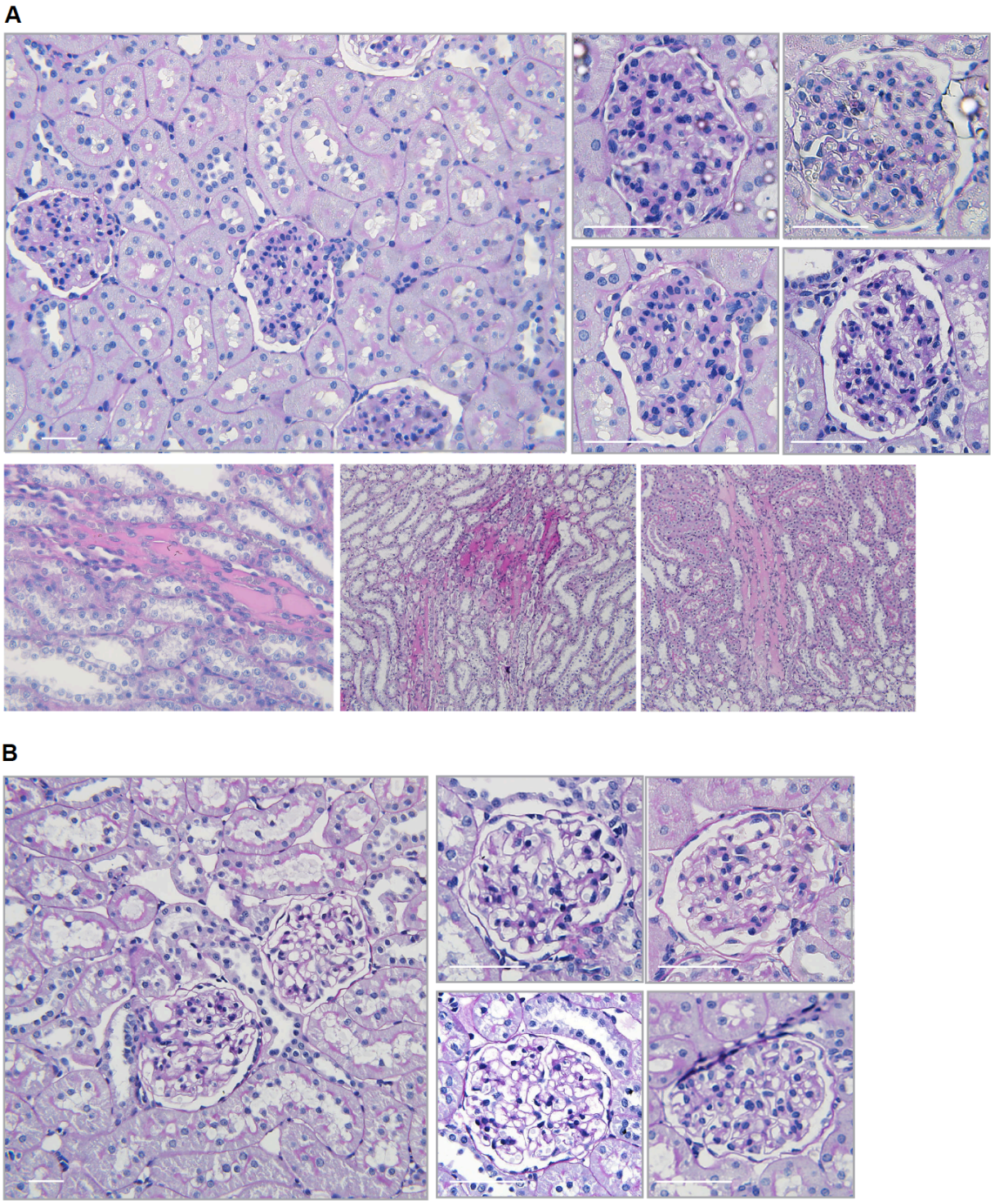

Figure S10. Renal histology features after 12 doses of injected poly-rIgA or mono-rIgA.
(A) Mesangial proliferation and matrix expansion were induced by 12 doses of poly-rIgA; two out of five rats had protein casts in tubulointerstitial areas. (B) Normal renal histology with mono-rIgA injections (12 doses). Scale bar: 50 μm.

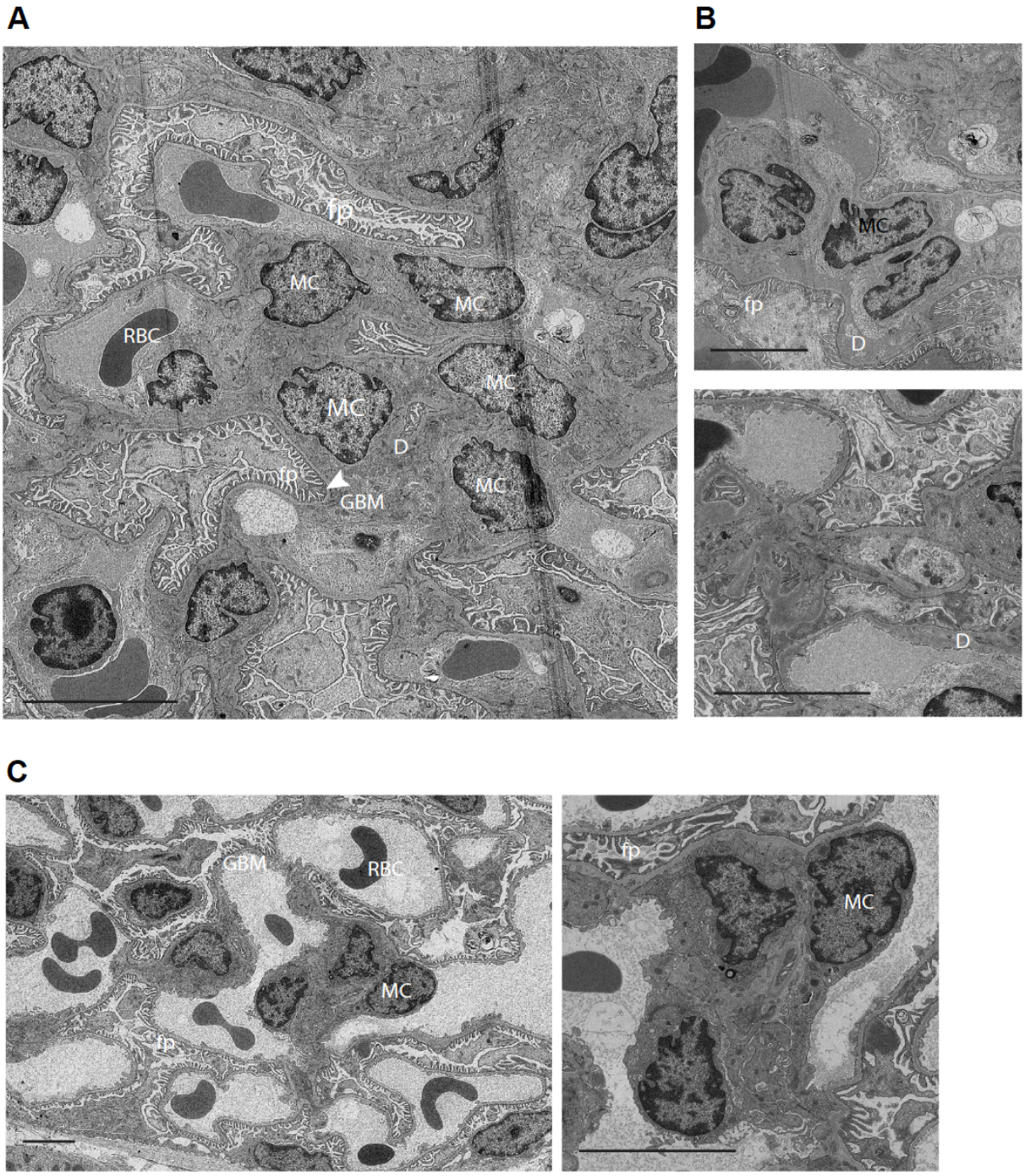

Figure S11. Electron microscopy of rat kidney tissue after 12 injections of poly-rIgA.
(A) TEM overview of the glomerulus shows regions populated by mesangial cells (MC); densities of irregular shapes could be seen between mesangial cells. Glomerular basement membrane (GBM; indicated by arrowheads), podocyte (pod), and foot processes (fp) appeared well preserved. RBC, red blood cell. Scale bar: 5 µm. (B) At higher magnification, electron dense materials (denoted by letter D) could be seen in the mesangial and subendothelial area. Foot processes (fp) appeared normal. (C) TEM showed normal kidney features in non-injected rats.

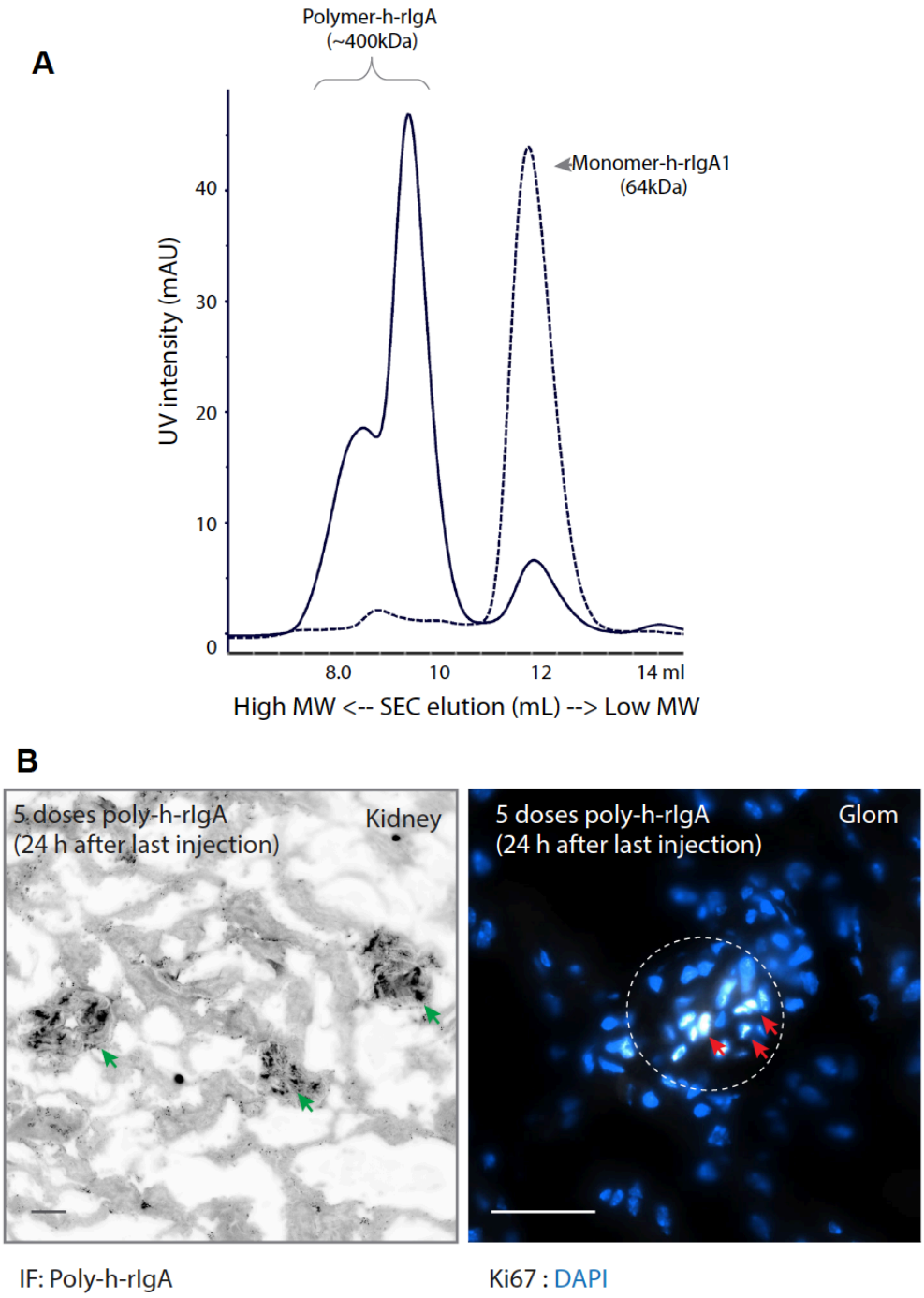

Figure S12. Human-derived poly-h-rIgA caused glomerular deposits in mice.
(A) Recombinant IgA Fc (h-rIgA) based on human IgA1 heavy chain sequence fused to an AviTag was produced in HEK293 cells. This h-rIgA was expected to contain glycan attachments. Following biotinylation, h-rIgA was induced for polymerization using streptavidin (SA) as described. SA induction caused an up(left)-shift in molecular weight (MW) as determined by size exclusion chromatography (SEC) (dotted line of mono-h-rIgA compared with solid line of poly-h-rIgA). (B) Injection of this poly-h-rIgA in mice for 5 consecutive days resulted in renal deposition detected by anti-IgA staining (left panel). The staining was concentrated in glomerulus areas (green arrows). Right panel: staining of the kidney sections with Ki67 showed positive nuclei (arrows) within the glomerulus (circle), indicating active cell proliferation.

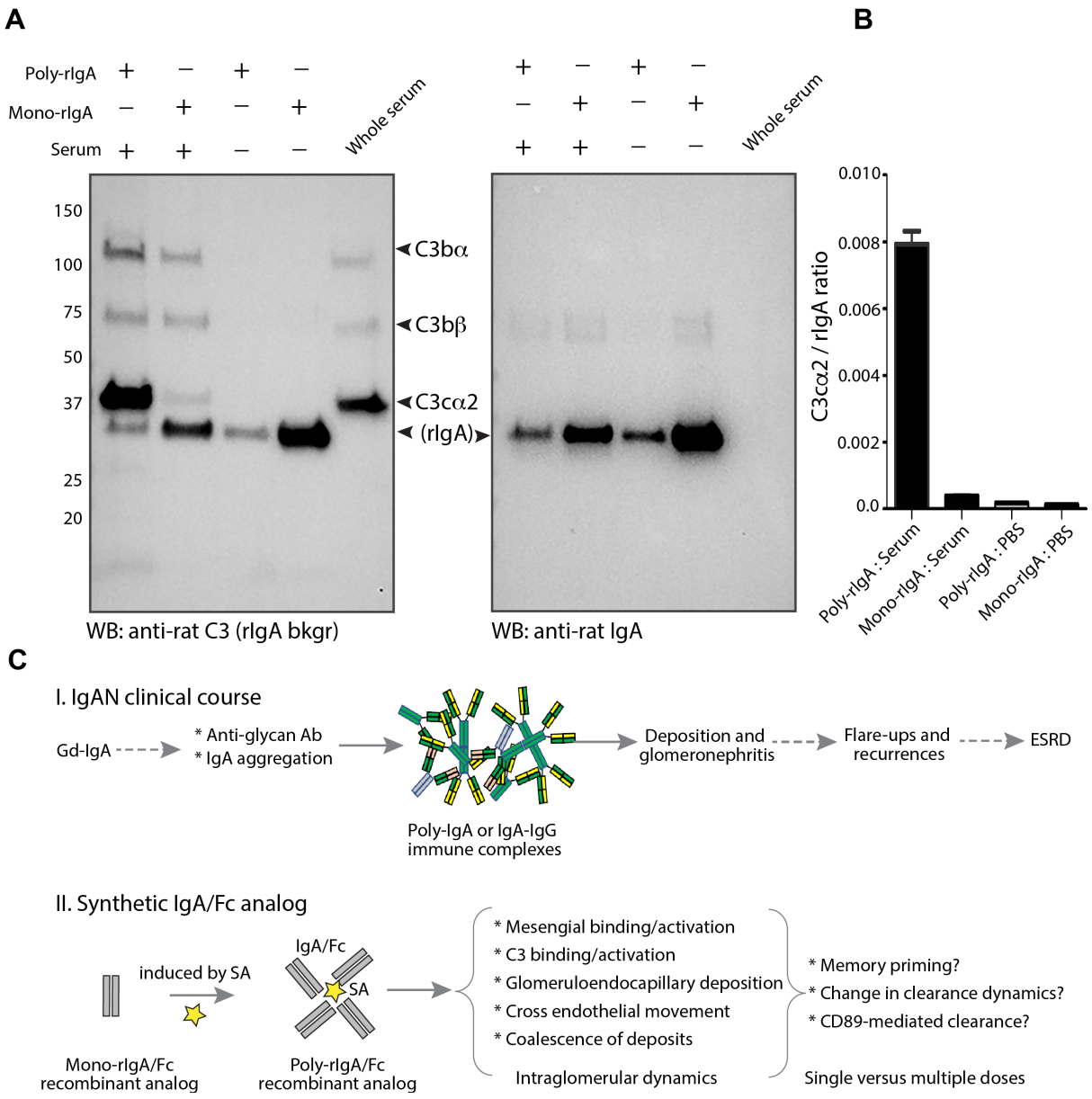

Figure S13. Poly-rIgA activates complement *in vitro*.
(A) Rat poly-rIgA and mono-rIgA were separately incubated with freshly harvested rat serum. These 6×His-tagged rIgA proteins were then immobilized by Ni^{2+}-NTA beads. Following elution with sample buffer, all proteins were resolved by SDS-PAGE, which was subsequently examined by western blotting with either anti-C3 or anti-IgA antibody (left and right panels, respectively). Several C3 bands were visible that corresponded to C3bα, C3bβ, and C3cα2. C3cα2 was prominently present with poly-rIgA. This was despite lower levels of poly-rIgA than mono-rIgA loading (right panel. Note: there was cross-reactive staining of r-IgA background/bkgr in the anti-rat C3 blot). The whole serum lane was a control. (B) C3cα2 to rIgA ratios were calculated, showing C3cα2 association with poly-rIgA. (C) A schematic model for the pathogenesis of poly-IgA immune complexes in IgAN as revealed by synthetic poly-rIgA analog. Top: modified four-hits hypothesis showing Gd-IgA at the beginning, followed by immune complex formation either via anti-glycan antibodies or intrinsic instability of Gd-IgA prone to self-aggregation, or both. Dotted arrows indicate unclear mechanism(s). In the synthetic IgA/Fc analog model (bottom panel), recombinant Fc of IgA was induced to multimerize via a biotin–streptavidin (SA) reaction. In this injection model of mono- versus poly-rIgA, the critical role of Fc multimerization was clearly demonstrated from several observations (in parentheses). This acute injection model, with the distinctions between single versus multiple injection, also raised new questions regarding the intraglomerular processing of IgA deposits, as to whether memory priming or other factors influence the kinetics of mesangial clearance.

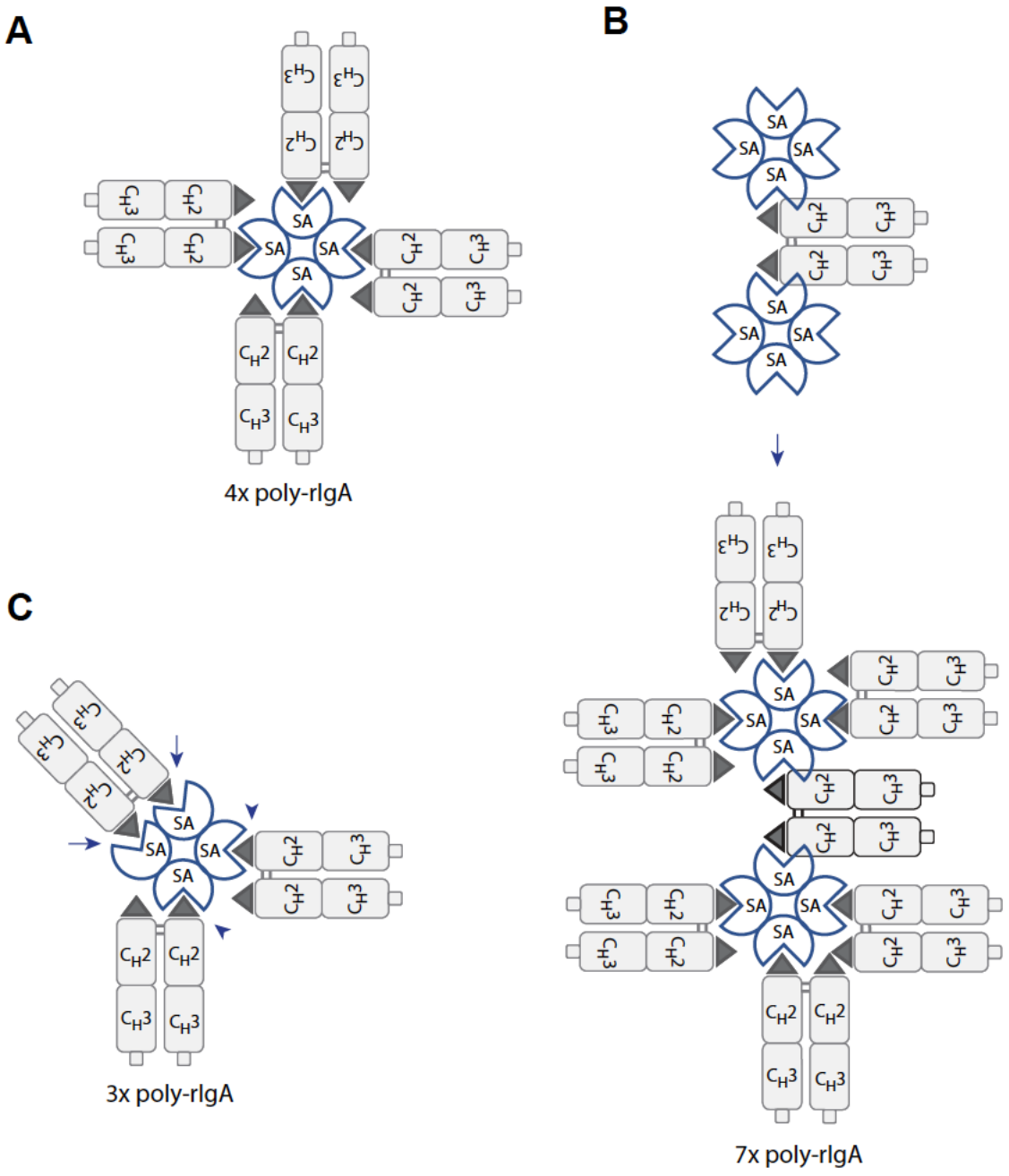

Figure S14. A variety of multimeric states of poly-rIgA are induced by streptavidin.
(A) Like its antibody counterpart of the IgA heavy chain, recombinant IgA Fc/CH2–CH3 naturally forms a dimer. Through the N-terminal biotin tag (solid triangle) of one of the two Fc chains, the duplex molecules interact with streptavidin (SA), which is a tetramer. Therefore, a 4× poly-rIgA is formed. (B) Similarly, each biotin tag of the rIgA duplex could also separately interact with two SAs, which further bind additional biotin-rIgA to form 7× poly-rIgA. (C) In the case of mixed binding modes between SA and the biotin tags, 3× poly rIgA could form.

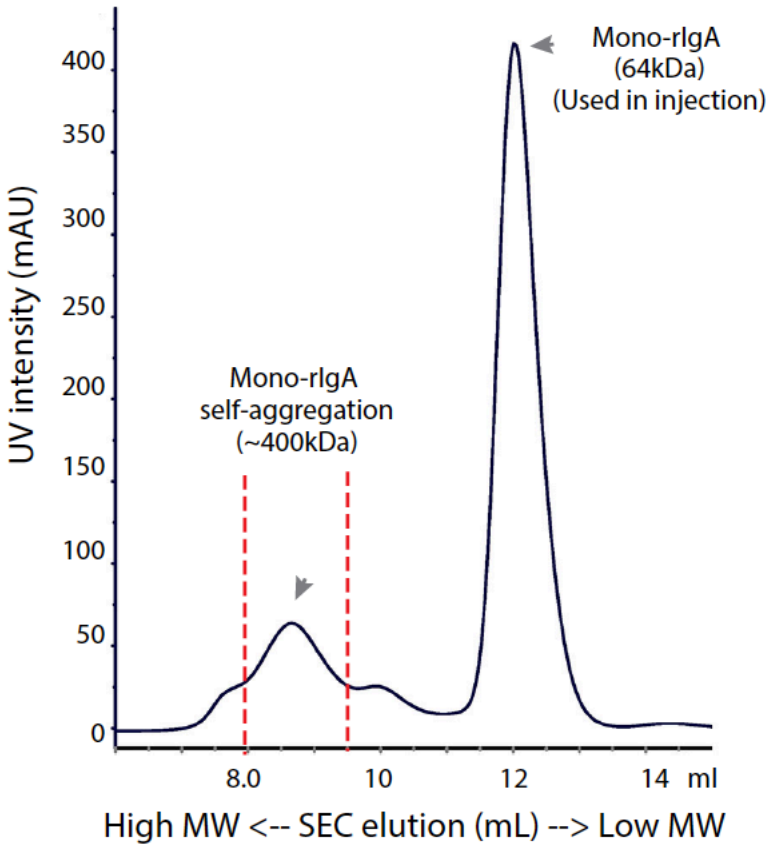

Figure S15. Recombinant mono-rIgA contained a small fraction of polymers from self-aggregation as detected by size exclusion chromatography (SEC).
By running size exclusion chromatography (SEC), a small fraction of self-aggregated poly-rIgA of ~400 kDa was detected (between dotted lines). For rat injection experiments, only the 64 kDa mono-rIgA was used.

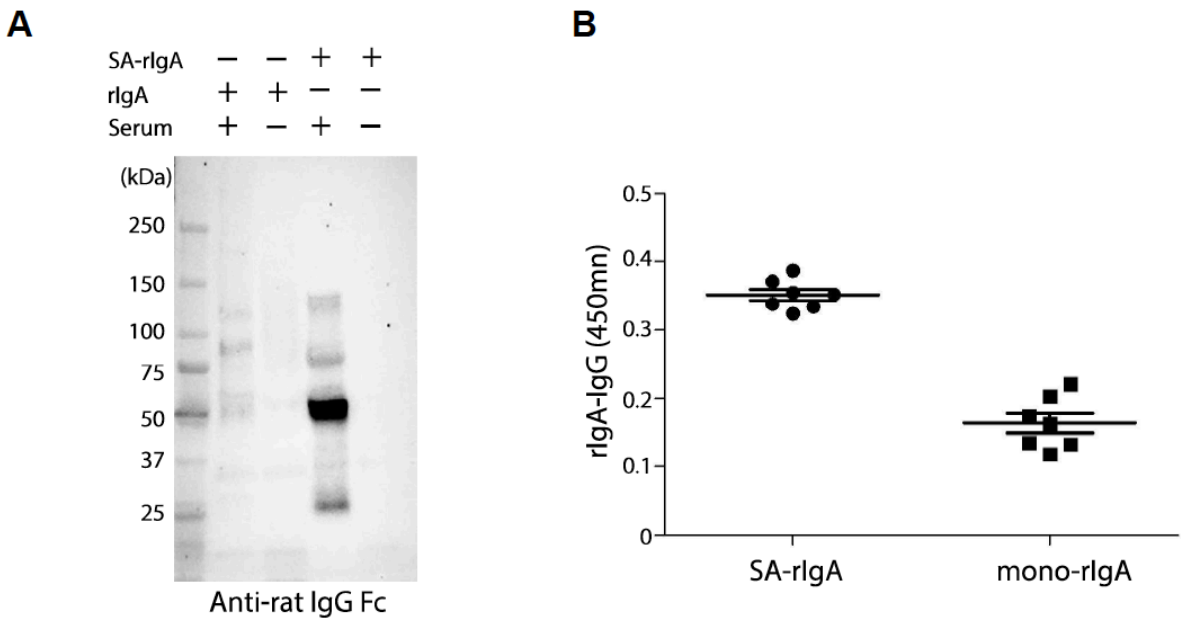

Figure S16. rIgA–IgG complex formation *in vitro*.
(A) Either SA-poly-rIgA or mono-rIgA was incubated with serum collected from naive rats. rIgA was purified by Nickel Magnetic beads, and proteins co-precipitated with rIgA were resolved using SDS-PAGE. Serum IgG was only detected in association with SA-poly-rIgA. (B) Higher binding of serum IgG was detected by ELISA in association with SA-poly-rIgA, compared with mono-rIgA.